PAPER

Check for updates

Calorimetric determination of the heat capacity function and absolute entropy of yttrium borohydride (Y(BH4)3) mechanochemically prepared

Konrad Burkmann, [ID] [a] Franziska Habermann, [ID] [a] Bianca Störr, [ID] [a] Jürgen Seidel, [a] Roman Gumeniuk, [ID] [b] Klaus Bohmhammel[a] and Florian Mertens [ID] *[ac]

Over the last two decades, complex metal hydrides have attracted attention in various fields such as chemical hydrogen storage, solid state electrolytes and superconductivity. In this context, we determined thermodynamic properties of the complex metal hydride Y(BH4)3. Yttrium borohydride was prepared by solid state metathesis yielding a mixture containing three equivalents lithium chloride beside the boranate. The benefit of the mechanochemical preparation procedure compared to the classical wet chemical one is to avoid the desolvation step which can lead to a partial decomposition of the hydride. The heat capacity of the compound as a function of the temperature covering a temperature range from 2 K to 370 K was determined using two different calorimetric techniques. Based on the heat capacity data, the standard entropy at 298.15 K was obtained. From the evaluation of the low temperature heat capacity region the Sommerfeld coefficient and the Debye temperature were derived.

Introduction

Even after many years of intensive research, complex hydrides continue to be the focus of current research in the fields of chemical hydrogen storage,[1–11] solid state electrolytes[12,13] and superconductivity.[14] Yttrium borohydride, Y(BH4)3, is a salt like borohydride with a theoretical total hydrogen content of about 9.1% and a decomposition temperature of 460 K[2]. Although reversibility has not been demonstrated yet for this material,[15] the compound may nevertheless be of interest because the dehydrogenation reaction is endothermic and, thus, the material may be suitable for rehydrogenation using a catalyst. It may also potentially be used as a component for modifying hydride mixtures by applying the concept of thermodynamic tuning to achieve reversibility for the overall reaction.[16,17] Therefore, reliable thermodynamic data are needed to predict the decomposition behaviour (*e.g.* decomposition temperature and products, equilibrium hydrogen pressure) of a given hydride mixture containing Y(BH4)3.

Several synthesis routes have been described for the synthesis of the α polymorph of Y(BH4)3 in the literature.[2,7] Nevertheless, solvent mediated or mechanochemically driven metathesis reactions without solvents using a ball mill are the two most common methods to synthesise Y(BH4)3 from YCl3 and an alkali metal borohydride (LiBH4 or NaBH4).[2,7] The reaction between yttrium chloride and lithium borohydride is given by eqn (1):

$$3LiBH_4 + YCl_3 \rightarrow Y(BH_4)_3 + 3LiCl \qquad (1)$$
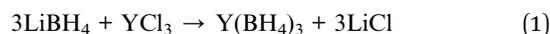
Jaroń and Grochala showed that the ball milling reaction did not take place by using sodium borohydride.[18] Several authors used ball milling for the synthesis of Y(BH4)3 as well[19–26] resulting in mixtures consisting of Y(BH4)3 and LiCl. For the solvent mediated metathesis DMS,[27] THF[18,28–30] or diethyl ether[15,31] were used. Besides the formation of stable solvent adducts, another problem is given by the solubility of the by-product LiCl in the used solvent,[15,32,33] except for DMS[29] in which LiCl is insoluble. Therefore, when using THF or diethyl ether as a reaction medium, it is advised to extract the product mixture with DMS to obtain a pure DMS-solvent adduct[29,31] or to use NaBH4 instead of LiBH4 as a reactant for the synthesis,[28] because NaCl is insoluble in diethyl ether and THF.[33] Certainly, the extraction step can also be applied when using the mechanochemical route. Any method that uses solvents must be complemented by a thermal desolvation step to obtain the pure Y(BH4)3.[29] However, very often uncontrolled hydrogen desorption occurs during the decomposition of the solvent complexes. In addition, the solvent itself can decompose during desolvation and thus contaminate the sample.

[a]Institut für Physikalische Chemie, TU Bergakademie Freiberg, Leipziger Straße 29, 09599 Freiberg, Germany. E-mail: florian.mertens@chemie.tu-freiberg.de; Tel: +49-3731-393737

[b]Institut für Experimentelle Physik, TU Bergakademie Freiberg, Leipziger Straße 23, 09599 Freiberg, Germany

[c]Zentrum für Effiziente Hochtemperatur-Stoffwandlung, TU Bergakademie Freiberg, Winklerstraße 5, 09599 Freiberg, Germany

Up to our best knowledge, only one publication addresses the determination of thermodynamic quantities of $Y(BH_4)_3$ so far. Lee *et al.* calculated the reaction enthalpies and reaction entropies for the decomposition of $Y(BH_4)_3$ into several yttrium borides using the Quantum-ESPRESSO density functional theory[34] from which we derived the enthalpies of formation and the absolute entropies of α-$Y(BH_4)_3$ and β-$Y(BH_4)_3$, resulting in the following values: $\Delta_F H$ (298.15 K) = −409.8 kJ mol^{-1} and S (298.15 K) = 149.4 J mol^{-1} K^{-1} for α-$Y(BH_4)_3$ and $\Delta_F H$ (298.15 K) = −405.9 kJ mol^{-1} and S (298.15 K) = 153.4 J mol^{-1} K^{-1} for the high temperature β polymorph of $Y(BH_4)_3$. The experimental determined temperature of the phase transition is about 454 K.[25,35,36] Nevertheless, no experimental values are available for both thermodynamic quantities.

The aim of our work is to determine experimentally the standard entropy of α-$Y(BH_4)_3$ using its measured heat capacity function. We used a solid state metathesis reaction leaving out the solvent extraction step that is often applied in complex metal hydride syntheses.[7,29] The latter to avoid decomposition and contamination with the solvent of the hydride halide mixtures ($Y(BH_4)_3$ + 3LiCl). To the best of our knowledge, this procedure has not been shown to be applicable to boranates and our study is the first to confirm that, if the composition of the mechanochemically produced mixtures is known, accurate thermodynamic data for the boranate can be obtained without separating the by-product prior to the respective calorimetric measurements. In future, this will further establish mechanochemistry as a simple and environmentally friendly method for the production of various hydrides, if their thermodynamic data are to be determined. This procedure is justified, because no double salts, like in the case of lanthanum borohydride forming $LaLi(BH_4)_3Cl$,[37,38] are formed and therefore the by-product LiCl can be assumed to be inert.

Experimental section

Materials

All handling and manipulation of the chemicals and the sample preparation for the measurements were performed in an argon (Nippon Gases, 5N) filled glove box with a gas circulation purifying system (H_2O and O_2 < 0.1 ppm) from MBRAUN.

Lithium borohydride ($LiBH_4$, Chemetall) and yttrium trichloride (YCl_3, Alfa Aesar, ultra dry, 99.99%) were used as received. Sapphire, (aluminium oxide, Al_2O_3) was used as reference material for the heat capacity measurements. A 25 μm thick copper foil (Cu, Alfa Aesar, 99.999%) was used to fold copper crucibles as containers for the samples used in the PPMS measurement.

Characterisation techniques

Powder X-ray diffraction (PXRD). The measurements were performed with a D2 Phaser from Bruker (5° to 85° 2θ, 0.05° 2θ steps, dwell time 1 s, 300 W X-ray power, $\lambda(K_\alpha)$ = 1.54184 nm) with a LYNXEYE detector. The powders were ground with a mortar and pestle and placed on a steel plate. To prevent oxidation of the samples during the measurement, the plate was covered with polyethylene foil.

Calorimetric heat capacity measurements. The heat capacities were measured in a temperature range from 2 K to 380 K based on the method described by ref. 4, 5, 8 and 9. The measurements in the low temperature region from 2 K to 300 K were conducted with a Physical Property Measurement System (PPMS, DynaCool-12, Quantum Design, USA) equipped with the heat capacity option, which is based on a relaxation technique described elsewhere.[39,40] The preparation of small copper crucibles containing the powdered sample is explained by ref. 41–43. To ensure a good thermal contact between the copper crucibles and the sample platform, Apiezon N grease was used, possessing besides a good thermal conductivity also a low heat capacity.[43–45] The PPMS software automatically computes the heat capacity, by subtracting the values of the addenda measurement (sample platform and grease) from the measured data of the sample (sample and crucible, sample platform and grease).[42] The heat capacity of the sample $C_{P,sample}$ is then calculated as the difference between the total measured specific heat $C_{P,total}$ and the specific heat of the copper crucible $C_{P,crucible}$, which is calculated from literature heat capacity data,[46] weighted according to their mass fractions.

$$C_{P,sample} = \frac{C_{P,total} - \omega_{crucible} \cdot C_{P,crucible}}{\omega_{sample}} \quad (2)$$

Furthermore, the same approach is used to obtain the specific heat of the $Y(BH_4)_3$ from the measured sample mixture of $Y(BH_4)_3$ + 3LiCl by subtracting the specific heat of LiCl from it using the data published by Shirley[47] and Moyer[48] for LiCl for temperatures lower than 300 K and from NIST[49] for temperatures higher than 300 K. The heat capacity measurements at temperatures higher than 280 K were performed in a DSC 111 from SETARAM, France, using the instrument software (Calisto, AKTS/SETARAM) to conduct the data evaluation and were inspired by the method already described elsewhere.[4–6,8,9,42,50–54] In detail, about 100 mg of the sample were filled into standard stainless steel sample vessels. Using a nickel sealing the vessels were crimped tightly. The nickel sealings and the vessels used for the sample, the reference and the blank were brought to an identical mass by hand polishing to avoid variations in the blank effects. A C_P-by-step method[55] based on four temperature steps (5 K, 3 K min^{-1}) each followed by an isothermal period of 30 min duration was conducted in the temperature range from 10 °C to 30 °C. After that, another step programme based on eight steps (10 K, 3 K min^{-1}) each also followed by an isothermal period of 30 min duration in the temperature range from 30 °C to 100 °C was performed. This procedure was used for the measurements of the sample, the reference (granular sapphire for the verification of the overall accuracy of the experiments) and the blank. Using the recommended reference heat capacity of sapphire published by Della Gatta *et al.*,[56] the specific heat of the sample were calculated *via* eqn (3).

$$\overline{C}_{P,sample} = \frac{\int_{t_i}^{t_{i+1}} \dot{Q}_{sample} dt - \int_{t_i}^{t_{i+1}} \dot{Q}_{blank} dt}{\int_{t_i}^{t_{i+1}} \dot{Q}_{ref} dt - \int_{t_i}^{t_{i+1}} \dot{Q}_{blank} dt} \cdot \frac{m_{ref}}{m_{sample}} \cdot \overline{C}_{P,ref} \quad (3)$$

$\bar{C}_{\mathrm{P,sample}}$ denotes the specific heat of the sample at the mean temperature of the ramp. The begin and end of the heat flow peaks $\dot{Q}$ are implied by the times t_i and t_{i+1}. The masses of the sample and reference material are given by m_{sample} and m_{ref}, respectively. Finally, $\bar{C}_{\mathrm{P,ref}}$ is used as the specific heat of the reference material at the mean temperature of the ramp. The molar heat capacity values can be derived by an multiplication with the molar mass of the $Y(BH_4)_3$ ($M_{Y(BH_4)_3}$).

Synthesis

Lithium borohydride and yttrium trichloride were ball milled in stoichiometric amounts (see reaction (1)) essentially following the published method from Ley *et al.*[27] A Fritsch Pulverisette 6 planetary ball mill equipped with a 80 mL-tungsten carbide (WC) crucible and three WC balls with an outer diameter of about 10 mm and 7.1 g of weight each were used. The milling programme applied consisted of 2 min milling followed by 2 min pause. This procedure was repeated for 179 times (total milling time of 6 h). A ball-to-powder-ratio of about 35 : 1 and rotational speed of 400 rpm were applied. The material was milled under protective atmosphere which was achieved by flooding the crucible with 1 bar of argon. After milling, the product mixture was removed from the crucible and stored for further investigations in the glove box.

Results and discussion

Phase purity of the synthesised samples using PXRD

From the absence of $LiBH_4$ and YCl_3 reflections in the diffractogram of the product mixture ($Y(BH_4)_3$ + 3LiCl), a complete conversion of the reactants can be inferred (Fig. 1).

Furthermore, there are no reflections of possible decomposition products such as YH_2, YH_3, B or other boron containing species visible indicating that there was no or negligible decomposition during milling, so the used procedure appears appropriate for the preparation of the compound.
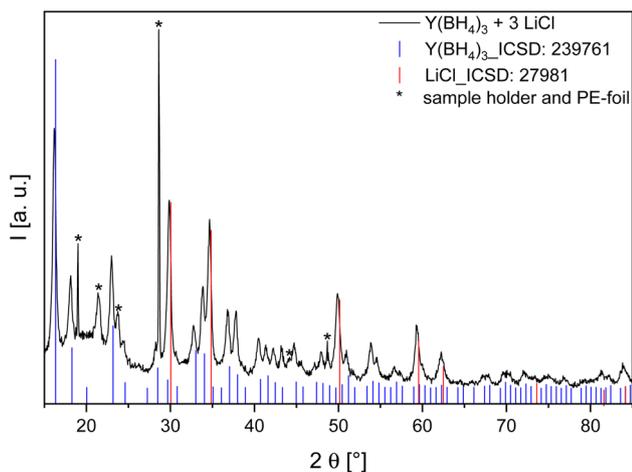

Fig. 1 PXRD of the product mixture after the metathesis reaction according to eqn (1). The reflections of the assigned phases were taken from the ICSD.[57]

Heat capacity function of $Y(BH_4)_3$

The experimental determination of the heat capacity of $Y(BH_4)_3$ was carried out over a broad temperature range from about 2 K to 370 K. To obtain the specific heat capacity values of $Y(BH_4)_3$ listed in Table 1 from the experimental values, the heat capacity of copper (crucible) and LiCl (by-product) were subtracted according to their mass fraction in the sample composition. The results of that calculation are presented in Fig. 2.

The inset graph in Fig. 2 displays the relative deviation of the experimental data from the respective fit function. The relative deviation of the measured values from the fits is mostly within ±1.5%, but the deviations are rising to maximal ±4.5% below a temperature of about 5 K and above a temperature of about 280 K. In order to keep the degree of the fitting polynomials both as low as possible and to ensure still satisfying fits, the temperature range of our heat capacity measurements was divided into five appropriate intervals. Similarly as in our recently published works[4-6,8,42,50-54] [$Ca(AlH_4)_2$, $Sr(BH_4)_2$], the heat capacities $C_P(T)$ were fitted then within these intervals using established polynomial functions.[58] The applied functions and the corresponding temperatures are given below.

$$0 \text{ K to } 5 \text{ K}: C_P = b \cdot T + e \cdot T^3 + f \cdot T^5 \tag{4}$$

$$5 \text{ K to } 17 \text{ K}: C_P = a + b \cdot T + c \cdot T^2 + d \cdot T^{-2} + e \cdot T^3 + g \cdot T^{-1} \tag{5}$$

$$17 \text{ K to } 100 \text{ K}: C_P = a + b \cdot T + c \cdot T^2 + d \cdot T^{-2} + e \cdot T^3 \tag{6}$$

$$100 \text{ K to } 230 \text{ K}: C_P = a + b \cdot T + c \cdot T^2 + d \cdot T^{-2} + e \cdot T^3 \tag{7}$$

$$230 \text{ K to } 380 \text{ K}: C_P = a + b \cdot T + c \cdot T^2 + d \cdot T^{-2} \tag{8}$$

The results for the fit coefficients and the fit quality parameters R^2 (coefficient of determination) and FitStdErr (fit standard error) are summarised in Table 2. The fits represent the experimental values with a deviation similar to the experimental standard uncertainty.

Applicability of Neumann–Kopp's rule to complex binding situations

Neumann–Kopp's rule is often used to calculate the heat unknown capacity of solid compounds from the heat capacities of the elements or smaller compounds forming the target compound.[59-62] In the case of borohydrides, however, this method is not applicable because hydrogen is gaseous under standard conditions. Nevertheless, it should be possible to estimate their heat capacity function using Neumann–Kopp's rule by calculating the specific heat function of BH_4 according to eqn (9) and using these values in combination with the specific heat of the metal of the studied metal borohydride to calculate its heat capacity according to eqn (10). The method was used for $Mg(BH_4)_2$ (ref. 61 and 63) and $Ca(BH_4)_2$.[61] Dematteis *et al.*[61] mentioned partly large deviations between the calculated and experimental values due to variations in the crystal structure and coordination number of the reactants. However, it remains unclear whether or not this method can be

Table 1 Experimental heat capacity values for $Y(BH_4)_3$ (M = 133.4341 g mol^{-1}) at p = 100 kPa

T [K]	C_P [J mol^{-1} K^{-1}]	T [K]	C_P [J mol^{-1} K^{-1}]	T [K]	C_P [J mol^{-1} K^{-1}]
2.0606	0.014475	8.9878	0.91862	16.132	3.9476
2.1413	0.015631	9.0881	0.95080	16.232	4.0055
2.2274	0.017200	9.1884	0.97756	16.333	4.0576
2.3149	0.018878	9.2883	1.0041	16.433	4.1196
2.4037	0.021122	9.3890	1.0356	16.534	4.1757
2.4938	0.023054	9.4893	1.0617	16.635	4.2365
2.5843	0.025405	9.5898	1.0927	16.735	4.2967
2.6782	0.027826	9.6902	1.1235	16.836	4.3564
2.7706	0.030499	9.7908	1.1540	16.936	4.4154
2.8635	0.033377	9.8935	1.1841	17.135	4.5323
2.9572	0.036619	9.9941	1.2141	22.171	7.6974
3.0517	0.040245	10.095	1.2491	27.115	11.301
3.1464	0.043804	10.195	1.2839	32.150	14.834
3.2414	0.047587	10.296	1.3131	37.185	18.269
3.3370	0.051741	10.396	1.3474	42.228	21.756
3.4332	0.056436	10.496	1.3814	47.270	25.309
3.5298	0.061063	10.597	1.4151	52.310	29.000
3.6266	0.066121	10.697	1.4537	57.355	32.649
3.7233	0.071602	10.797	1.4920	62.394	36.422
3.8203	0.077023	10.897	1.5249	67.437	40.117
3.9177	0.083336	10.998	1.5627	72.478	43.696
4.0155	0.089187	11.098	1.5950	77.519	47.354
4.1131	0.096278	11.199	1.6322	82.560	50.983
4.2109	0.10351	11.299	1.6692	87.605	54.165
4.3114	0.11039	11.399	1.7110	92.645	57.312
4.4094	0.11826	11.499	1.7473	97.679	60.687
4.5078	0.12619	11.599	1.7834	102.72	64.238
4.6060	0.13486	11.700	1.8242	105.73	66.244
4.7047	0.14348	11.800	1.8649	115.76	73.770
4.8031	0.15253	11.901	1.9050	125.85	80.581
4.9019	0.16270	12.001	1.9450	135.90	86.421
5.0007	0.17256	12.101	1.9846	145.99	92.704
5.0996	0.18273	12.202	2.0290	156.08	98.812
5.1985	0.19347	12.302	2.0679	166.19	104.51
5.2978	0.20505	12.402	2.1117	176.30	110.05
5.3966	0.21646	12.503	2.1551	186.47	115.26
5.4956	0.22863	12.603	2.1930	196.59	120.25
5.5948	0.24118	12.704	2.2357	206.72	125.19
5.6945	0.25413	12.804	2.2832	216.82	131.33
5.7936	0.26769	12.904	2.3252	226.93	137.14
5.8931	0.28123	13.005	2.3720	237.02	142.90
5.9926	0.29621	13.105	2.4184	247.11	148.37
6.0921	0.31006	13.205	2.4645	257.17	153.60
6.1916	0.32517	13.306	2.5049	267.27	158.99
6.2915	0.33963	13.406	2.5554	277.36	165.66
6.3908	0.35666	13.507	2.6003	285.98	176.07
6.4906	0.37244	13.607	2.6447	286.21	179.95
6.5901	0.38877	13.707	2.6940	287.45	173.64
6.6898	0.40518	13.808	2.7376	291.13	176.92
6.7894	0.42601	13.908	2.7860	291.35	183.82
6.8891	0.44148	14.009	2.8339	296.08	177.07
6.9887	0.46201	14.109	2.8869	296.29	187.76
7.0887	0.48236	14.210	2.9339	297.56	177.53
7.1884	0.49736	14.310	2.9858	301.09	185.29
7.2885	0.51738	14.410	3.0373	301.30	189.24
7.3878	0.53729	14.511	3.0831	310.37	191.46
7.4878	0.55697	14.611	3.1336	310.38	192.50
7.5876	0.58171	14.712	3.1837	320.44	197.12
7.6876	0.60106	14.812	3.2385	320.45	199.20
7.7876	0.62543	14.913	3.2876	330.49	204.91
7.8876	0.64442	15.013	3.3414	330.50	206.57
7.9877	0.66842	15.127	3.4012	340.30	211.37
8.0875	0.69226	15.226	3.4544	340.53	216.02

Table 1 (Contd.)

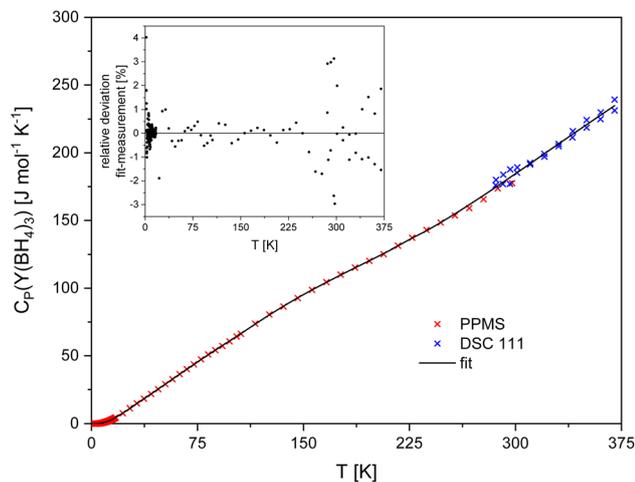| T [K]	C_P [J mol^{-1} K^{-1}]	T [K]	C_P [J mol^{-1} K^{-1}]	T [K]	C_P [J mol^{-1} K^{-1}]
8.1878	0.71588	15.327	3.5066	350.31	218.64
8.2872	0.73936	15.427	3.5584	350.32	224.28
8.3874	0.76780	15.528	3.6149	360.10	224.91
8.4874	0.78565	15.628	3.6656	360.33	229.90
8.5875	0.81370	15.729	3.7210	370.11	231.34
8.6873	0.84156	15.830	3.7759	370.12	239.35
8.7875	0.86919	15.930	3.8302		
8.8876	0.89662	16.031	3.8892		

Fig. 2 Temperature dependence of the molar heat capacity C_P of $Y(BH_4)_3$ in the temperature range from about 2 K to 370 K. The inset shows the relative deviation of the experimental data from the fit function.

used for transition metal boranates, as there has been no application to this class of compounds so far.

$$C_{P,BH_4} = C_{P,MBH_4} - C_{P,M} \text{ with M = Li, Na} \quad (9)$$

$$C_{P,M(BH_4)_x} = C_{P,M} + x \cdot C_{P,BH_4} \quad (10)$$

Table 3 lists the coefficients for the Maier Kelley[58] heat capacity function polynomials of Y, Li and LiBH$_4$ shown below:

$$C_P = A + B \cdot T + C \cdot T^{-2} + D \cdot T^3 + E \cdot T^3 + F \cdot T^{-1} \quad (11)$$

The coefficients for the C_P range below 300 K for Y and LiBH$_4$ are derived from the fits of given literature values and the ones for Li are obtained from its G function. Above room temperature all values were taken from the HSC 5.1 database. All data used were validated by comparing various literature sources (as far as possible) and seem to posses high reliability. Respective references are shown in Table 3.

The comparison between our experimental values and those derived from the described method using LiBH$_4$ are presented in Fig. 3. The use of NaBH$_4$ as reported by Dematteis et al.[61] was

not reasonably applicable because of the presence of a phase transition at 189.9 K.[68]

The inset in Fig. 3 displays the deviation of the values of the experimental fit curve from the one calculated by the Neumann–Kopp rule. The deviation between both curves is significant and exceeds in a wide temperature range 10%. Towards high temperatures the slope of the Neumann–Kopp curve decreases so that both curves intersect at about 335 K. Similar behaviour has been found in other systems[59,60,62] and was attributed to factors that are not reflected in the Neumann–Kopp rule such as magnetism and anharmonic effects[60] or the formation of Schottky defects.[62]

In general Neumann–Kopp's rule is reasonably applicable for simple compounds (alloys), whose elements show in pure form the same crystal structure as the compounds to be described. In cases where the compound possesses complex subunits, it is necessary not only to consider the binding situation within the subunit but also that of the subunit in the target compound.[59,61] In the case of the calculation of the heat capacity of $Y(BH_4)_3$ according to eqn (9) and (10), the requirements that the crystal structures of the components and the binding situation of the subunits should be the same is not fulfilled. Li crystallises in the body centred cubic W type structure (space group 229),[69] Y in the hexagonal Mg type structure (space group 194),[70] LiBH$_4$ in a orthorhombic structure (space group 62)[31] and $Y(BH_4)_3$ in a cubic structure (space group 205).[31]

In the literature, the influence of the thermal expansion of the compounds, among other things, was used for the extension of the Neumann–Kopp approximation in order to obtain more realistic C_P values. Kumar et al. and Leitner et al. applied the extended Neumann–Kopp method to CaHCl and CaHBr[59] and mixed oxides,[60] respectively and obtained significant improvements. Unfortunately, this procedure is currently not applicable because of the missing thermal expansion coefficient for $Y(BH_4)_3$.

By the integration of the conventional Neumann–Kopp C_P function divided by the temperature in the range from 5 K to 300 K, a value of the standard entropy of S° (300 K) = 183.8 J mol^{-1} K^{-1} was derived. This value differs about 9% from the experimental one determined in this study (vide infra). This result is a further indication of the limitation in regard to the use of the Neumann–Kopp approximation.

Based on the given explanations, the Neumann–Kopp rule can be seen as a rough estimation method and cannot replace

Table 2 Fitted coefficients of the heat capacity functions of $Y(BH_4)_3$ (M = 133.4341 g mol⁻¹)

T interval [K]	a [J mol⁻¹ K⁻¹]	b [J mol⁻¹ K⁻²]	c [J K mol⁻¹]	d [J mol⁻¹ K⁻³]	e [J mol⁻¹ K⁻⁴]	f [J mol⁻¹ K⁻⁶]	g [J mol⁻¹]	R^2	FitStdErr
0 to 5	0	$1.4814 \cdot 10^{-3}$	0	0	$1.2216 \cdot 10^{-3}$	$4.0961 \cdot 10^{-6}$	0	1.0000	$2.6436 \cdot 10^{-4}$
5 to 17	$6.0668 \cdot 10^{0}$	$-8.0424 \cdot 10^{-1}$	$6.0859 \cdot 10^{-2}$	$3.8147 \cdot 10^{1}$	$-8.6660 \cdot 10^{-4}$	0	$-2.4058 \cdot 10^{1}$	1.0000	$3.1382 \cdot 10^{-3}$
17 to 100	$-6.5064 \cdot 10^{0}$	$5.9847 \cdot 10^{-1}$	$2.2764 \cdot 10^{-3}$	$5.4218 \cdot 10^{1}$	$-1.3670 \cdot 10^{-5}$	0	0	0.9999	$1.5525 \cdot 10^{-1}$
100 to 230	$-1.4167 \cdot 10^{2}$	$2.7555 \cdot 10^{0}$	$-1.1015 \cdot 10^{-2}$	$2.0107 \cdot 10^{5}$	$1.8536 \cdot 10^{-5}$	0	0	0.9999	$2.6848 \cdot 10^{-1}$
230 to 370	$-2.2501 \cdot 10^{2}$	$1.5227 \cdot 10^{0}$	$-9.3269 \cdot 10^{-4}$	$3.3004 \cdot 10^{6}$	0	0	0	0.9879	$3.0988 \cdot 10^{0}$

reliable experimental data. From our findings for $Y(BH_4)_3$ its application appears also not recommended for precise thermodynamic calculations regarding other transition metal boranates that have not yet been prepared/investigated.

Calculation of the standard entropy, entropy of formation and of the enthalpy change

The calculation of the standard entropy values $S°$ was carried out using the fitted polynomials for the heat capacity values in the temperature range of 2 K to 370 K using eqn (12).

$$S°(T) = \int_0^{T_{final}} \frac{C_P}{T} dT \qquad (12)$$

The value for the standard entropy $S°$ at 298.15 K was determined to be $S°$ (298.15 K) = (168.9 ± 5.1) J mol⁻¹ K⁻¹, which is considerably higher than the value reported by Lee *et al.* for the room temperature α-phase of $Y(BH_4)_3$ (149.4 J mol⁻¹ K⁻¹) derived *via* DFT calculations.[34] All calculated values of $S°$ are presented in Table 4. In addition, the molar standard entropy of formation $\Delta_F S°$ has been calculated from eqn (13) resulting in a value of $\Delta_F S°$ (298.15 K) = −677.7 J mol⁻¹ K⁻¹. The values for the standard entropy of yttrium, boron and hydrogen were taken from the HSC database.[65]

$$\Delta_F S° = S°_{Y(BH_4)_3} - S°_Y - 3 \cdot S°_B - 6 \cdot S°_{H_2} \qquad (13)$$

For the calculation of the change in molar enthalpy $\Delta H_0^T = H(T) - H(0)$ the heat capacity functions were integrated according to eqn (14).

$$\Delta H_0^T = H(T) - H(0) = \int_0^{T_{final}} C_P dT \qquad (14)$$

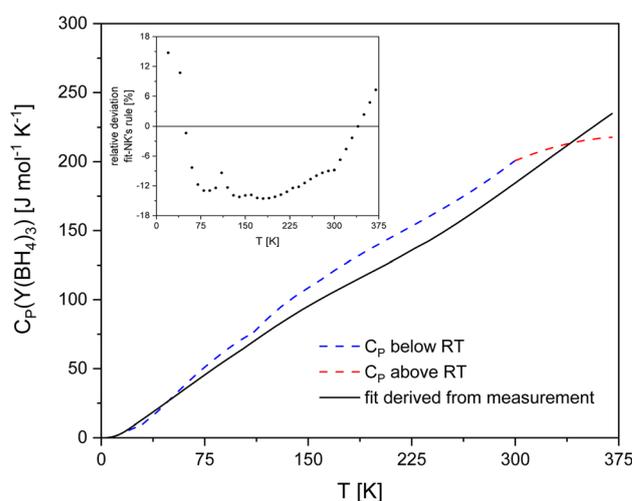**Fig. 3** Comparison between the heat capacity of $Y(BH_4)_3$ derived from our measurements (black solid line) and the one computed by applying Neumann–Kopp's rule according to ref. 61 and 63 (red dashed line: values below room temperature; blue dashed line: values above room temperature). The inset displays the relative deviation between the experimental values and the ones from the Neumann–Kopp rule.

© 2025 The Author(s). Published by the Royal Society of Chemistry

Table 3 Coefficients of the heat capacity functions according to eqn (11). The temperature ranges for the compounds were taken from the given sources

Compound	T range [K]	A [J mol^{-1} K]	B [J mol^{-1} K^{-2}]	C [J K mol^{-1}]	D [J mol^{-1} K^{-3}]	E [J mol^{-1} K^{-4}]	F [J mol^{-1}]
Y	20 to 300 (ref. 64)	$2.831 \cdot 10^{-1}$	$4.842 \cdot 10^{-2}$	$1.098 \cdot 10^{4}$	$-2.899 \cdot 10^{-4}$	$4.886 \cdot 10^{-7}$	$-1.093 \cdot 10^{3}$
	300 to 1755 (ref. 65)	$2.390 \cdot 10^{1}$	$7.620 \cdot 10^{-3}$	$3.130 \cdot 10^{4}$	0	0	0
Li	20 to 105 (ref. 66)	$-1.615 \cdot 10^{0}$	$2.728 \cdot 10^{-2}$	$2.814 \cdot 10^{2}$	$2.085 \cdot 10^{-3}$	$-8.382 \cdot 10^{-6}$	0
	105 to 170 (ref. 66)	$4.839 \cdot 10^{2}$	$-7.341 \cdot 10^{0}$	$-7.569 \cdot 10^{5}$	$4.272 \cdot 10^{-2}$	$-8.641 \cdot 10^{-5}$	0
	170 to 300 (ref. 66)	$-4.353 \cdot 10^{1}$	$5.752 \cdot 10^{-1}$	$2.167 \cdot 10^{5}$	$-1.791 \cdot 10^{-3}$	$2.024 \cdot 10^{-6}$	0
	300 to 453 (ref. 65)	$3.895 \cdot 10^{1}$	$-7.098 \cdot 10^{-2}$	$-3.202 \cdot 10^{5}$	$1.193 \cdot 10^{-4}$	0	0
LiBH$_4$	20 to 300 (ref. 67)	$-4.903 \cdot 10^{1}$	$9.717 \cdot 10^{-1}$	$-6.683 \cdot 10^{3}$	$-3.169 \cdot 10^{-3}$	$4.538 \cdot 10^{-6}$	$9.822 \cdot 10^{2}$
	300 to 400 (ref. 65)	$-4.671 \cdot 10^{1}$	$6.779 \cdot 10^{-1}$	$1.728 \cdot 10^{5}$	$-8.409 \cdot 10^{-4}$	0	0

The calculated values of $\Delta H_0{}^T$ divided by the temperature are given in Table 4 as well as the Φ parameter, which can be computed by eqn (15).

$$\Phi = \Delta S_0{}^T - \frac{\Delta H_0{}^T}{T} \qquad (15)$$

$\Delta S_0{}^T$ is equal to the absolute standard entropy $S(T)°$ (see eqn (12)). However, it is necessary to carry out reliable calorimetric measurements to obtain the enthalpy of formation, which will then be used to construct the Gibbs energy function with the data obtained in this study.

Table 4 Molar thermodynamic functions of Y(BH$_4$)$_3$ ($M = 133.4341$ g mol^{-1}) at selected temperatures between 5 K to 380 K and pressure of $p = 100$ kPa

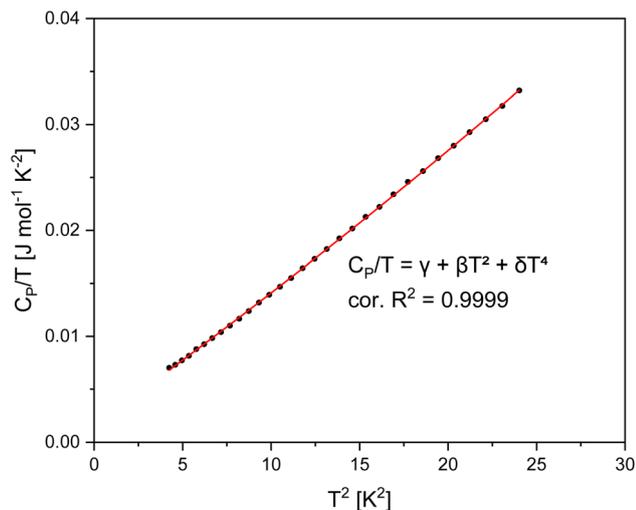| T [K]	C_P [J mol^{-1} K^{-1}]	$\Delta S_0{}^T$ [J mol^{-1} K^{-1}]	$\Delta H_0{}^T/T$ [J mol^{-1} K^{-1}]	Φ [J mol^{-1} K]	T [K]	C_P [J mol^{-1} K^{-1}]	$\Delta S_0{}^T$ [J mol^{-1} K^{-1}]	$\Delta H_0{}^T/T$ [J mol^{-1} K^{-1}]	Φ [J mol^{-1} K]
5	0.17291	0.06087	0.044012	0.016855	195	119.53	106.40	59.589	46.807
10	1.2194	0.44076	0.32539	0.11538	200	122.135	109.45	61.120	48.335
15	3.3375	1.3011	0.94792	0.35321	205	124.767	112.50	62.640	49.863
20	6.3997	2.6616	1.9117	0.74991	210	127.434	115.54	64.151	51.391
25	9.7512	4.4478	3.1428	1.3051	215	130.150	118.57	65.654	52.918
30	13.188	6.5283	4.5295	1.9988	220	132.927	121.60	67.151	54.444
35	16.687	8.8233	6.0157	2.8076	225	135.778	124.61	68.644	55.970
40	20.234	11.283	7.5708	3.7117	230	138.715	127.63	70.136	57.495
45	23.815	13.872	9.1765	4.6957	235	141.089	130.63	71.615	59.019
50	27.421	16.568	10.821	5.7474	240	144.024	133.64	73.093	60.543
55	31.039	19.351	12.494	6.8570	245	147.061	136.64	74.571	62.065
60	34.659	22.207	14.190	8.0167	250	150.189	139.64	76.052	63.586
65	38.271	25.124	15.904	9.2201	255	153.397	142.64	77.537	65.107
70	41.863	28.092	17.630	10.462	260	156.675	145.65	79.027	66.627
75	45.426	31.102	19.364	11.737	265	160.016	148.67	80.524	68.147
80	48.949	34.146	21.104	13.042	270	163.410	151.69	82.027	69.666
85	52.423	37.218	22.844	14.374	275	166.851	154.72	83.538	71.185
90	55.836	40.311	24.582	15.729	280	170.331	157.76	85.057	72.704
95	59.178	43.420	26.316	17.105	285	173.846	160.81	86.584	74.223
100	62.440	46.539	28.041	18.498	290	177.389	163.86	88.119	75.742
105	65.914	49.668	29.760	19.908	295	180.956	166.92	89.662	77.261
110	69.443	52.816	31.483	21.332	298.15	183.213	168.86	90.638	78.219
115	72.934	55.980	33.210	22.770	300	184.541	169.99	91.213	78.781
120	76.367	59.157	34.937	24.220	305	188.141	173.07	92.773	80.302
125	79.729	62.342	36.662	25.681	310	191.751	176.16	94.340	81.823
130	83.012	65.534	38.381	27.152	315	195.369	179.26	95.915	83.345
135	86.211	68.727	40.094	28.633	320	198.990	182.37	97.497	84.868
140	89.326	71.919	41.797	30.122	325	202.611	185.48	99.087	86.392
145	92.358	75.106	43.488	31.618	330	206.231	188.60	100.683	87.917
150	95.310	78.287	45.167	33.121	335	209.845	191.73	102.28	89.443
155	98.189	81.460	46.831	34.629	340	213.453	194.86	103.89	90.970
160	101.00	84.622	48.480	36.142	345	217.050	198.01	105.51	92.498
165	103.75	87.772	50.113	37.659	350	220.636	201.15	107.13	94.028
170	106.45	90.909	51.731	39.179	355	224.209	204.31	108.75	95.559
175	109.11	94.034	53.332	40.701	360	227.766	207.47	110.38	97.092
180	111.74	97.144	54.918	42.226	365	231.305	210.64	112.01	98.625
185	114.34	100.24	56.489	43.752	370	234.826	213.81	113.65	100.160
190	116.93	103.32	58.045	45.279					

Fig. 4 Plot of C_P/T versus T^2 of $Y(BH_4)_3$ in the temperature range from 0 K to 5 K.

Heat capacity at low temperatures

In the low temperature range between about 2 K and 5 K a three parameter fit function was applied (see eqn (16)). Fig. 4 displays the corresponding C_P/T-*vs.*-T^2 plot showing a high value of the coefficient of determination (R^2) for the applied temperature range of the low temperature fit.

$$C_P = C_{P,elec} + C_{P,vib} = \gamma \cdot T + \beta \cdot T^3 + \delta \cdot T^5 \tag{16}$$

Usually, the linear term with the Sommerfeld coefficient γ is attributed to the electrical conductivity of metals and related compounds.[50–54,71,72] However, there are also publications taking into account the electronic contribution to the heat capacity for non conductive materials. Loos *et al.*[42] observed this behaviour for lithium iron phosphate and explained it with the existence of electronic states in structural defects. Defects in the crystal structure of the synthesised $Y(BH_4)_3$ that may potentially contribute to the heat capacity even at low temperatures can be assumed to be present because of the preparation by ball milling.[71,73,74] Habermann *et al.* found that the linear term is also required for a sufficient fit of the heat capacity values at low temperatures for various metal alanates produced by ball milling.[4,5,8] The need of a linear term for nonmetallic, insulating compounds in the low temperature range due to the existence of vacancies in the lattice was also postulated by Schliesser and Woodfield.[74] The parameters β and δ in eqn (16) are related to the lattice vibration contribution to the heat capacity in terms of the Debye theory.[71,72]

A value of $\gamma = (1.48 \pm 0.01) \cdot 10^{-3}$ J mol^{-1} K^{-2} is obtained for the Sommerfeld coefficient, which is comparable to that one of metals.[71] As mentioned above the phenomenon is common if structural defects are present in the sample.[42,74] For the lattice vibration parameter, the value of $\beta = (1.22 \pm 0.01) \cdot 10^{-3}$ J mol^{-1} K^{-4} was determined. A Debye temperature of $\Theta_D = (294.2 \pm 1.1)$ K was calculated using eqn (17) with the given number of atoms

per formula unit of $n = 16$ for $Y(BH_4)_3$. This value represents the excitation of low energy acoustic phonons (lattice vibrations), shown in the phonon density of states diagram calculated by Lee *et al.*[34]

$$\Theta_D = \sqrt[3]{\frac{12 \cdot \pi^4 \cdot n \cdot R}{5 \cdot \beta}} \tag{17}$$

The coefficient of the T^5 term of the lattice contribution in eqn (16) was found to be $\delta = (4.09 \pm 0.44) \cdot 10^{-6}$ J mol^{-1} K^{-6}.

Conclusions

In the presented work, the heat capacity function of $Y(BH_4)_3$ between 2 K and 370 K was derived from mechanochemically prepared samples containing $Y(BH_4)_3$ + 3LiCl. The mixture was used as received after ball milling for the heat capacity measurements to avoid a partial decomposition of the boranate during the common solvent extraction. Our investigations show that this method is a convincing way for the determination of thermodynamic data from hydrides in mixtures obtained by mechanochemistry.

The measurement at low temperatures allows the determination of the absolute standard entropy resulting in a value of $S^\circ (298.15\ K) = (168.9 \pm 5.1)$ J mol^{-1} K^{-1} and a Debye temperature of $\Theta_D = (294.2 \pm 1.1)$ K. Despite the fact that the material is non-metallic, a comparably high value of $\gamma = (1.48 \pm 0.01) \cdot 10^{-3}$ J mol^{-1} K^{-2} was obtained for the Sommerfeld coefficient. This fact seems to be not unusual for mechanochemically prepared complex metal hydrides.

The absolute standard entropy derived from the measured data deviates significantly from the value of this quantity determined *via* DFT calculations in the literature. Given the determined uncertainty of the measurements of less than 5%, the obtained values appear to be more convincing. Although not surprising, however often applied, the estimate of the heat capacity *via* the modified Neumann–Kopp rule with the inclusion of complex subunits, in the presented case BH_4, did not yield a satisfactory agreement with experimental findings.

Further investigations should address the determination of the enthalpy of formation as well as the understanding of the complex decomposition process. It is necessary to obtain thermodynamic values for possible decomposition intermediates to perform thermodynamic calculations on their existence during the decomposition process of $Y(BH_4)_3$. Applying this knowledge hopefully a deeper understanding of the potential use of $Y(BH_4)_3$ for reversible hydrogen storage concerning thermodynamic tuning strategies will be reached.

Data availability

The data supporting this article have been included as part of the manuscript. In detail, Table 1 gives all measured heat capacity values depending on the measurement temperature. The data to calculate the curves in Fig. 3 are calculated with the

heat capacity values found in the literature, whereby all references indicated in Table 3.

Author contributions

Conflicts of interest

There are no conflicts to declare.

Acknowledgements

Notes and references

1 K. Suárez-Alcántara, J. R. Tena-Garcia and R. Guerrero-Ortiz, *Materials*, 2019, **12**, 2724–2787.

2 K. Suárez-Alcántara and J. R. T. García, *Materials*, 2021, **14**, 2561.

3 F. Habermann, K. Burkmann, B. Hansel, B. Störr, C. Schimpf, J. Seidel, M. Bertau and F. Mertens, *Dalton Trans.*, 2023, **52**, 4880–4890.

4 F. Habermann, A. Wirth, K. Burkmann, B. Störr, J. Seidel, R. Gumeniuk, K. Bohmhammel and F. Mertens, *ChemPhysChem*, 2024, **25**, e202300748.

5 F. Habermann, A. Wirth, K. Burkmann, J. Kraus, B. Störr, H. Stöcker, J. Seidel, J. Kortus, D. C. Meyer, R. Gumeniuk, K. Bohmhammel and F. Mertens, *RSC Mechanochem.*, 2024, submitted.

6 K. Burkmann, F. Habermann, E. Schumann, J. Kraus, B. Störr, H. Schmidt, E. Brendler, J. Seidel, K. Bohmhammel, J. Kortus and F. Mertens, *New J. Chem.*, 2024, **48**, 2743–2754.

7 Z. Cao, F. Habermann, K. Burkmann, M. Felderhoff and F. Mertens, *Hydrogen*, 2024, **5**, 241–279.

8 F. Habermann, K. Burkmann, J. Kraus, B. Störr, J. Seidel, K. Bohmhammel, J. Kortus, R. Gumeniuk and F. Mertens, *J. Alloys Compd.*, 2024, **980**, 173476.

9 K. Burkmann, A. Demmer, F. Habermann, B. Hansel, B. Störr, J. Seidel, R. Gumeniuk, M. Bertau, K. Bohmhammel and F. Mertens, *J. Therm. Anal. Calorim.*, 2025, DOI: **10.1007/s10973-025-14085-z**.

10 C. Milanese, T. R. Jensen, B. C. Hauback, C. Pistidda, M. Dornheim, H. Yang, L. Lombardo, A. Zuettel, Y. Filinchuk, P. Ngene, P. E. de Jongh, C. E. Buckley, E. M. Dematteis and M. Baricco, *Int. J. Hydrogen Energy*, 2019, **44**, 7860–7874.

11 E. M. Dematteis, M. B. Amdisen, T. Autrey, J. Barale, M. E. Bowden, C. E. Buckley, Y. W. Cho, S. Deledda, M. Dornheim, P. de Jongh, J. B. Grinderslev, G. Gizer, V. Gulino, B. C. Hauback, M. Heere, T. W. Heo, T. D. Humphries, T. R. Jensen, S. Y. Kang, Y.-S. Lee, H.-W. Li, S. Li, K. T. Møller, P. Ngene, S.-I. Orimo, M. Paskevicius, M. Polanski, S. Takagi, L. Wan, B. C. Wood, M. Hirscher and M. Baricco, *Prog. Energy*, 2022, **4**, 032009.

12 R. Černý, F. Murgia and M. Brighi, *J. Alloys Compd.*, 2022, **895**, 162659.

13 C. Comanescu, *Materials*, 2022, **15**, 2286.

14 S. Di Cataldo and L. Boeri, *Phys. Rev. B*, 2023, **107**, L060501.

15 Y. Yan, H.-W. Li, T. Sato, N. Umeda, K. Miwa, S.-i. Towata and S.-I. Orimo, *Int. J. Hydrogen Energy*, 2009, **34**, 5732–5736.

16 J. J. Vajo, F. Mertens, C. C. Ahn, R. C. Bowman and B. Fultz, *J. Phys. Chem. B*, 2004, **108**, 13977–13983.

17 J. J. Vajo, S. L. Skeith and F. Mertens, *J. Phys. Chem. B*, 2005, **109**, 3719–3722.

18 T. Jaroń and W. Grochala, *Dalton Trans.*, 2010, **39**, 160–166.

19 F. C. Gennari, *Int. J. Hydrogen Energy*, 2012, **37**, 18895–18903.

20 T. Jaroń, W. Koźmiński and W. Grochala, *Phys. Chem. Chem. Phys.*, 2011, **13**, 8847–8851.

21 T. Jaroń and W. Grochala, *Dalton Trans.*, 2011, **40**, 12808–12817.

22 T. Jaroń, W. Wegner, K. J. Fijałkowski, P. J. Leszczyński and W. Grochala, *Chem.–Eur. J.*, 2015, **21**, 5689–5692.

23 Y. Nakamori, H.-W. Li, M. Matsuo, K. Miwa, S. Towata and S. Orimo, *J. Phys. Chem. Solids*, 2008, **69**, 2292–2296.

24 K. Park, H.-S. Lee, A. Remhof, Y.-S. Lee, Y. Yan, M.-Y. Kim, S. J. Kim, A. Züttel and Y. W. Cho, *Int. J. Hydrogen Energy*, 2013, **38**, 9263–9270.

25 D. B. Ravnsbaek, Y. Filinchuk, R. Cerný, M. B. Ley, D. Haase, H. J. Jakobsen, J. Skibsted and T. R. Jensen, *Inorg. Chem.*, 2010, **49**, 3801–3809.

26 T. Sato, K. Miwa, Y. Nakamori, K. Ohoyama, H.-W. Li, T. Noritake, M. Aoki, S.-i. Towata and S.-I. Orimo, *Phys. Rev. B:Condens. Matter Mater. Phys.*, 2008, **77**, 104114.

27 M. B. Ley, M. Paskevicius, P. Schouwink, B. Richter, D. A. Sheppard, C. E. Buckley and T. R. Jensen, *Dalton Trans.*, 2014, **43**, 13333–13342.

28 M. Mostajeran, E. Ye, S. Desgreniers and R. T. Baker, *Chem. Mater.*, 2017, **29**, 742–751.

29 B. Richter, J. B. Grinderslev, K. T. Møller, M. Paskevicius and T. R. Jensen, *Inorg. Chem.*, 2018, **57**, 10768–10780.

30 A. Brukl and K. Rossmanith, *Monatsh. Chem.*, 1959, **90**, 481–487.

31 E. Roedern, Y.-S. Lee, M. B. Ley, K. Park, Y. W. Cho, J. Skibsted and T. R. Jensen, *J. Mater. Chem. A*, 2016, **4**, 8793–8802.

32 K. Rossmanith and E. Muckenhuber, *Monatsh. Chem.*, 1961, **92**, 600–604.

33 H. C. Brown, Y. M. Choi and S. Narasimhan, *Inorg. Chem.*, 1982, **21**, 3657–3661.

34 Y.-S. Lee, J.-H. Shim and Y. W. Cho, *J. Phys. Chem. C*, 2010, **114**, 12833–12837.

35 C. Frommen, N. Aliouane, S. Deledda, J. E. Fonneløp, H. Grove, K. Lieutenant, I. Llamas-Jansa, S. Sartori, M. H. Sørby and B. C. Hauback, *J. Alloys Compd.*, 2010, **496**, 710–716.

36 R. Černý and P. Schouwink, *Acta Crystallogr., Sect. B:Struct. Sci., Cryst. Eng. Mater.*, 2015, **71**, 619–640.

37 M. B. Ley, S. Boulineau, R. Janot, Y. Filinchuk and T. R. Jensen, *J. Phys. Chem. C*, 2012, **116**, 21267–21276.

38 S. P. GharibDoust, M. Brighi, Y. Sadikin, D. B. Ravnsbæk, R. Černý, J. Skibsted and T. R. Jensen, *J. Phys. Chem. C*, 2017, **121**, 19010–19021.

39 C. A. Kennedy, M. Stancescu, R. A. Marriott and M. A. White, *Cryogenics*, 2007, **47**, 107–112.

40 J. C. Lashley, M. F. Hundley, A. Migliori, J. L. Sarrao, P. G. Pagliuso, T. W. Darling, M. Jaime, J. C. Cooley, W. L. Hults, L. Morales, D. J. Thoma, J. L. Smith, J. Boerio-Goates, B. F. Woodfield, G. R. Stewart, R. A. Fisher and N. E. Phillips, *Cryogenics*, 2003, **43**, 369–378.

41 S. Loos, *Dissertation*, TU Bergakademie Freiberg, Freiberg, 2014.

42 S. Loos, D. Gruner, M. Abdel-Hafiez, J. Seidel, R. Hüttl, A. U. Wolter, K. Bohmhammel and F. Mertens, *J. Chem. Thermodyn.*, 2015, **85**, 77–85.

43 Q. Shi, C. L. Snow, J. Boerio-Goates and B. F. Woodfield, *J. Chem. Thermodyn.*, 2010, **42**, 1107–1115.

44 C. A. Swenson, *Rev. Sci. Instrum.*, 1999, **70**, 2728–2731.

45 W. Schnelle, J. Engelhardt and E. Gmelin, *Cryogenics*, 1999, **39**, 271–275.

46 G. K. White and S. J. Collocott, *J. Phys. Chem. Ref. Data*, 1984, **13**, 1251–1257.

47 D. A. Shirley, *J. Am. Chem. Soc.*, 1960, **82**, 3841–3843.

48 D. F. Moyer, *J. Phys. Chem. Solids*, 1965, **26**, 1459–1462.

49 W. G. Mallard and P. J. Linstrom, *NIST Chemistry WebBook: NIST Standard Reference Database Number 69, Datenbank*, 2022, **https://webbook.nist.gov/**.

50 D. Thomas, M. Abdel-Hafiez, T. Gruber, R. Hüttl, J. Seidel, A. U. Wolter, B. Büchner, J. Kortus and F. Mertens, *J. Chem. Thermodyn.*, 2013, **64**, 205–225.

51 D. Thomas, M. Zeilinger, D. Gruner, R. Hüttl, J. Seidel, A. U. Wolter, T. F. Fässler and F. Mertens, *J. Chem. Thermodyn.*, 2015, **85**, 178–190.

52 F. Taubert, S. Schwalbe, J. Seidel, R. Hüttl, T. Gruber, R. Janot, M. Bobnar, R. Gumeniuk, F. Mertens and J. Kortus, *Int. J. Mater. Res.*, 2017, **108**, 942–958.

53 F. Taubert, J. Seidel, R. Hüttl, M. Bobnar, R. Gumeniuk and F. Mertens, *J. Chem. Thermodyn.*, 2018, **116**, 323–329.

54 F. Taubert, J. Seidel, R. Hüttl, M. Bobnar, R. Gumeniuk and F. Mertens, *J. Chem. Thermodyn.*, 2019, **130**, 119–128.

55 S. M. Sarge, G. W. H. Höhne and W. Hemminger, *Calorimetry: Fundamentals, Instrumentation and Applications*, Wiley-VCH Verlag, Weinheim, Germany, 2014.

56 G. Della Gatta, M. J. Richardson, S. M. Sarge and S. Stølen, *Pure Appl. Chem.*, 2006, **78**, 1455–1476.

57 G. Bergerhoff and I. D. Brown, *Crystallographic Databases*, International Union of Crystallography, Chester, 1987.

58 C. G. Maier and K. K. Kelley, *J. Am. Chem. Soc.*, 1932, **54**, 3243–3246.

59 S. S. Kumar, S. Ghosh, M. Sahu and R. Ganesan, *J. Chem. Sci.*, 2019, **131**, 1–7.

60 J. Leitner, P. Voňka, D. Sedmidubský and P. Svoboda, *Thermochim. Acta*, 2010, **497**, 7–13.

61 E. M. Dematteis, S. R. Jensen, T. R. Jensen and M. Baricco, *J. Chem. Thermodyn.*, 2020, **143**, 106055.

62 T. Zienert and O. Fabrichnaya, *Calphad*, 2019, **65**, 177–193.

63 E. R. Pinatel, E. Albanese, B. Civalleri and M. Baricco, *J. Alloys Compd.*, 2015, **645**, S64–S68.

64 G. A. Berezovskij, I. E. Paukov, G. S. Burkhanov and O. D. Chistyakov, *Zh. Fiz. Khim.*, 1989, **63**, 3141–3143.

65 A. Roine, *HSC Chemistry*, 2002, **https://www.hsc-chemistry.com/**.

66 P. Wang, A. Kozlov, D. Thomas, F. Mertens and R. Schmid-Fetzer, *Intermetallics*, 2013, **42**, 137–145.

67 N. C. Hallett and H. L. Johnston, *J. Am. Chem. Soc.*, 1953, **75**, 1496–1497.

68 H. L. Johnston and N. C. Hallett, *J. Am. Chem. Soc.*, 1953, **75**, 1467–1468.

69 M. R. Nadler and C. P. Kempier, *Anal. Chem.*, 1959, **31**, 2109.

70 F. H. Spedding, A. H. Daane and K. W. Herrmann, *Acta Crystallogr.*, 1956, **9**, 559–563.

71 E. Gopal, *Specific Heats at Low Temperatures*, Springer, New York, NY, 1966.

72 A. Tari, *The Specific Heat of Matter at Low Temperatures*, Imperial College Press, London and River Edge, NJ, 2003.

73 R. Felten, U. Umhofer, U. Rauchschwalbe and G. Weber, *J. Magn. Magn. Mater.*, 1985, **47–48**, 39–41.

74 J. M. Schliesser and B. F. Woodfield, *Phys. Rev. B:Condens. Matter Mater. Phys.*, 2015, **91**, 024109.